Ultrasonics Sonochemistry 35 (2017) 103–111

Contents lists available at ScienceDirect

Ultrasonics Sonochemistry

journal homepage: www.elsevier.com/locate/ultson

Effect of ultrasound on the function and structure of a membrane protein: The case study of photosynthetic Reaction Center from *Rhodobacter sphaeroides*

Vincenzo De Leo [a,b,*], Lucia Catucci [a,b], A. Evelyn Di Mauro [b], Angela Agostiano [a,b], Livia Giotta [c], Massimo Trotta [b], Francesco Milano [b]

[a] Department of Chemistry, University of Bari, Via Orabona 4, 70126 Bari, Italy
[b] CNR-IPCF Institute for Physical and Chemical Processes, Bari Unit, Via Orabona 4, 70126 Bari, Italy
[c] Department of Biological and Environmental Sciences and Technologies, University of Salento, SP Lecce-Monteroni, 73100 Lecce, Italy

ARTICLE INFO

Article history:
Received 15 July 2016
Received in revised form 5 September 2016
Accepted 6 September 2016
Available online 7 September 2016

Keywords:
Ultrasound
Denaturation
Integral membrane proteins
Reaction Center
Rhodobacter sphaeroides

ABSTRACT

Ultrasounds are used in many industrial, medical and research applications. Properties and function of proteins are strongly influenced by the interaction with the ultrasonic waves and their bioactivity can be lost because of alteration of protein structure. Surprisingly, to the best of our knowledge no study was carried out on Integral Membrane Proteins (IMPs), which are responsible for a variety of fundamental biological functions. In this work, the photosynthetic Reaction Center (RC) of the bacterium *Rhodobacter sphaeroides* has been used as a model for the study of the ultrasound-induced IMP denaturation. Purified RCs were suspended in i) detergent micelles, in ii) detergent-free buffer and iii) reconstituted in liposomes, and then treated with ultrasound at 30 W and 20 kHz at increasing times. The optical absorption spectra showed a progressive and irreversible denaturation in all cases, resulting from the perturbation of the protein scaffold structure, as confirmed by circular dichroism spectra that showed progressive alterations of the RC secondary structure. Charge recombination kinetics were studied to assess the protein photoactivity. The lifetime for the loss of RC photoactivity was 32 min in detergent micelles, ranged from 3.8 to 6.5 min in the different proteoliposomes formulations, and 5.5 min in detergent-free buffer. Atomic force microscopy revealed the formation of large RC aggregates related to the sonication-induced denaturation, in agreement with the scattering increase observed in solution.

1. Introduction

Ultrasonic treatments are widely utilized in research, industry and medicine [1]. A non-exhaustive list of possible uses includes many food processing applications (e.g. cleaning of equipment, homogenization of milk, inactivation of microorganisms, product modification [2–4]), pharmaceutical techniques (microencapsulation procedure, liposome preparation, drug release [5–7]), biotechnological processes (e.g. for extracting metabolites and bioactive compounds from plant or animal material [8,9]), and medicine applications (such as imaging, dentistry, liposuction, tumor ablation and kidney stone disruption [7]). Ultrasounds are also used in the investigation of protein conformational disorders such as Alzheimer's and prion diseases, where proteins are altered and misfolded to form aggregates [10,11].

Ultrasonic waves are elastic waves or stress waves with frequencies higher than 20 kHz. In a medium exposed to ultrasound, the formation of gas- or vapor-filled bubbles occurs, in a phenomenon called cavitation [7]. Bubbles can continuously oscillate in response to an oscillating pressure, with a radius that varies about an equilibrium value (Stable cavitation) [7,12], or oscillate with increasingly larger amplitudes until the outward expansion exceeds a limiting value, upon which the bubbles grow suddenly and then collapse violently (Inertial cavitation) [7,13]. The cavitation events, and the collapses of the bubbles in particular, produce shock waves, micro-streaming, and shear stresses [7,12]. Inertial cavitation also induces the formation of free radicals via thermal dissociation of water [14].

The interaction of the ultrasonic radiation with living material therefore, inevitably affects the structure and properties of biomolecules in a way that depend mainly on the duration and intensity

* Corresponding author at: Department of Chemistry, University of Bari, Via Orabona 4, 70126 Bari, Italy.
E-mail address: v.deleo@ba.ipcf.cnr.it (V. De Leo).

http://dx.doi.org/10.1016/j.ultsonch.2016.09.007
1350-4177/

of exposure. The damage that proteins can potentially receive from such extreme treatments include denaturation via two main mechanisms. The first one involves conformational perturbation, (e.g. unfolding process due to the rupture of the hydrogen bonds and Van der Waals interactions in the polypeptide chains and/or aggregation via noncovalent interactions); the second one occurs through chemical reactions (such as hydrolysis, oxidation, deamidation, β-elimination, etc.) [15]. In both cases sonication could denature proteins, through the formation of liquid-gas interfaces, local heating effects, mechanical/sheer stresses, and free radical reactions [1,16,17]. Bioactivity is lost as a result of alteration of protein secondary and tertiary structure [18].

Despite numerous applications of ultrasound in medical, pharmaceutical and industrial fields, the details of ultrasound-induced damage of proteins, and more generally of biomolecules, remain poorly characterized owing to the potentially complex mechanisms involved [1].

A certain number of studies on soluble proteins such as lysozyme [1,6], trypsin [18], bovine serum albumin (BSA), myoglobin, superoxide dismutase, Tm0979, hisactophilin [1], β2-microglobulin [19], whey protein [20] and on enzymes of biotechnological interest [21] was carried out. To date, to the best of our knowledge, no study was carried out on Integral Membrane Proteins (IMPs). This is undoubtedly due to the higher functional and structural complexity of IMPs as compared to water-soluble globular proteins. Moreover purified IMPs are not generally available on the market and they need to be reconstructed in a membrane-like environment to stabilize a correct spatial structure and to support their functional activity in solution [22]. IMPs, however, represent over 25% of the proteins encoded in the genome of higher animals and are responsible for a variety of fundamental biological functions [23,24]. They also play a crucial role in the cell communication, intercellular recognition, signal transduction, cell energetics, and transport processes through the membrane [22,24].

The purpose of the present work was to gain insight into the effects of ultrasound on IMPs. We studied the photosynthetic Reaction Center (RC) from the bacterium *Rhodobacter sphaeroides* as IMP model protein. Indeed, the availability of crystallographic structure at very high-resolution makes RC an ideal reference protein for the study of general principles of membrane protein architecture and structure-function relationships. Furthermore, in addition to absorbance signals related to tryptophan and tyrosine, RC features a rich electronic spectrum in the visible-NIR region due to the presence of several cofactors that facilitate the study of the protein. Finally, RC can be easily reconstituted in the membrane-mimicking environments represented by liposomes. All these features make the RC an ideal candidate to study sonication-induced denaturation phenomena on IMPs.

2. Materials and methods

2.1. Materials

All chemicals were purchased with the highest purity available and used without further purification. The reagent grade salts for the 50 mM K-phosphate, 100 mM KCl (pH 7.0) buffer solutions, sodium cholate (SC), N,N-dimethyldodecylamine-N-oxide (LDAO), cholesterol (CH), diphosphatidylglycerol (cardiolipin, CL), and G-50 Sephadex Superfine were purchased from Sigma. Phosphatidylcholine (PC) was from Lipoid.

2.2. RC protein purification

RCs were isolated from *Rhodobacter sphaeroides* strain R-26.1 grown photoheterotrophically under anaerobic conditions as previously described [25]. Protein purity was checked using the ratio of the absorbance at 280 and 802 nm (A_{280}/A_{802}), which was kept below 1.3, and the ratio of the absorbance at 760 and 865 nm (A_{760}/A_{865}), which was kept equal to or lower than 1 [26]. Protein was stored frozen at −20 °C in the final buffer Tris-HCl 20 mM, EDTA 1 mM, LDAO 0.025% (w/v), named TLE buffer.

2.3. RC reconstitution in liposomes

Reaction Center reconstitution in liposomes was accomplished by the micelle-to-vesicle transition (MVT) method as previously reported [27]. Briefly, 2.6 mg of total phospholipids were dissolved in a chloroform solution. Such solution was carefully dried on the walls of a conical vial under a gentle N_2 stream to form an evenly distributed film of phospholipids. A volume of 500 µl of a 4% sodium cholate solution in K-phosphate buffer (KPi) 50 mM, KCl 100 mM, pH 7.0 was added to the film and lipids were solubilized by 10–20 cycles one-second sonication to form a homogenous translucent solution. The appropriate amount of RC (45 µM stock solution) was added to this solution, vigorously shacked, stored for 15 min at 4 °C and finally loaded onto a 15 cm Sephadex G-50 column previously equilibrated with KPi 50 mM, KCl 100 mM, pH 7.0 for the size exclusion chromatography (SEC) step. The RC-proteoliposomes elute after the void volume of ∼1.5 mL in a 1 mL fraction.

2.4. Ultrasound treatment

A volume of 5 mL of micellar RC or RC-liposome suspensions, at total protein concentration of 1 µM, was sonicated in a glass vial, using an ultrasonic horn (3.5 mm diameter, Branson Sonifier® 250, Danbury, CT) operating at 20 kHz. The instrument, which can deliver a maximum power of 200 W, was set to 30 W in pulsed mode and duty cycle control 40%. During ultrasound treatment, the vial containing the sample was kept in an ice/water bath to prevent overheating phenomena.

2.5. UV–Vis–NIR spectroscopy

Absorption measurements were performed by means of a UV/vis/NIR Cary 5000 Spectrophotometer (Varian). Scattering contribution to absorption spectra was subtracted using the software "Spekwin32" (F. Menges, Version 1.72.2, 2016, http://www.effem-m2.de/spekwin/).

2.6. Charge recombination kinetics

Charge recombination (CR) kinetics were recorded at 865 nm using a kinetic spectrophotometer of local design implemented with an Hamamatsu R928 photomultiplier and an Hamamatsu Xenon flash lamp (pulse length ∼100 µs) used for RC photoexcitation. Data were collected onto a Digital Oscilloscope (Tektronics TKS3200) and trace deconvolution was performed using a C-code developed in our lab. All measurements were performed at 25 °C unless diversely indicated. The decay traces were recorded up to complete recovery of the photo-bleaching. The absorbance changes were measured assuming as starting value the baseline recorded before the flash [28].

2.7. Circular dichroism spectroscopy

Circular dichroism (CD) spectra were recorded at 25 °C using a Jasco J-810 spectropolarimeter equipped with a Peltier thermostat. Measurements were conducted with a 0.1 cm path length quartz cell, a 10 nm/min scan rate and a 0.2 nm bandwidth. Spectra were an average of 3 scans from 200 to 250 nm. The spectrum of 50 mM

K-phosphate, 100 mM KCl (pH 7.0) buffer was used as a blank and subtracted from the average three spectra to obtain a corrected spectrum for each sample.

2.8. Atomic force microscopy studies

Topography Atomic Force Microscopy (AFM) measurements were performed by means of a PSIA XE-100 SPM system operating in tapping mode, in air and at room temperature. A silicon AFM probe (Park Systems) with a cantilever having a force constant of 42 N m^{-1} and a resonance frequency of 330 kHz was used. Micrographs were collected by sampling the surface at a scan rate of 1 Hz, with a resolution of 256 × 256 pixels. AFM micrographs were processed by using the XEI software.

3. Results and discussion

The photosynthetic Reaction Center from the strain R26 of the bacterium *R. sphaeroides* is a membrane-spanning protein composed of three subunits named L, M, and H. The subunits L and M are related by a 2-fold symmetry axle and contain five transmembrane alpha helixes each. The subunit H contains only one alpha helix structurally used to lock its globular portion to the rest of the protein. Nine cofactors are non-covalently bound to protein scaffold: two ubiquinone-10 (UQ_{10}), a non-heme Fe^{2+} ion, two bacteriopheophytins (BPhe) and four bacteriochlorophylls (BChl), two of which forming a functional dimer (D) (Fig. 1 A, B). A 2-fold symmetry axle joining the dimer and the Fe^{2+} ion and coinciding with the one of the L and M subunits, relates the cofactors, which are arranged in two branches named A and B. Cofactors have a A or B subscript according to the protein branch they are located. The UQ_{10} molecules in the two branches are commonly named as Q_A and Q_B.

The purified RC is surrounded by a toroid of detergent molecules, typically LDAO [29], preventing its precipitation in water. RC is the pivotal element in the photosynthetic process since its dimer, upon photon absorption, is able to shuttle an electron through the chain of pigments in the A branch, eventually reaching the final acceptor Q_B (Fig. 1 C, D). In this way, the radiant energy coming from the solar light is trapped in the charge-separated state $D^+Q_B^-$, and eventually transformed into useful chemical energy.

The RC is an ideal model protein for the study of structure-function relationships. Indeed its structure is one of the best characterized among the membrane proteins, with an available resolu-

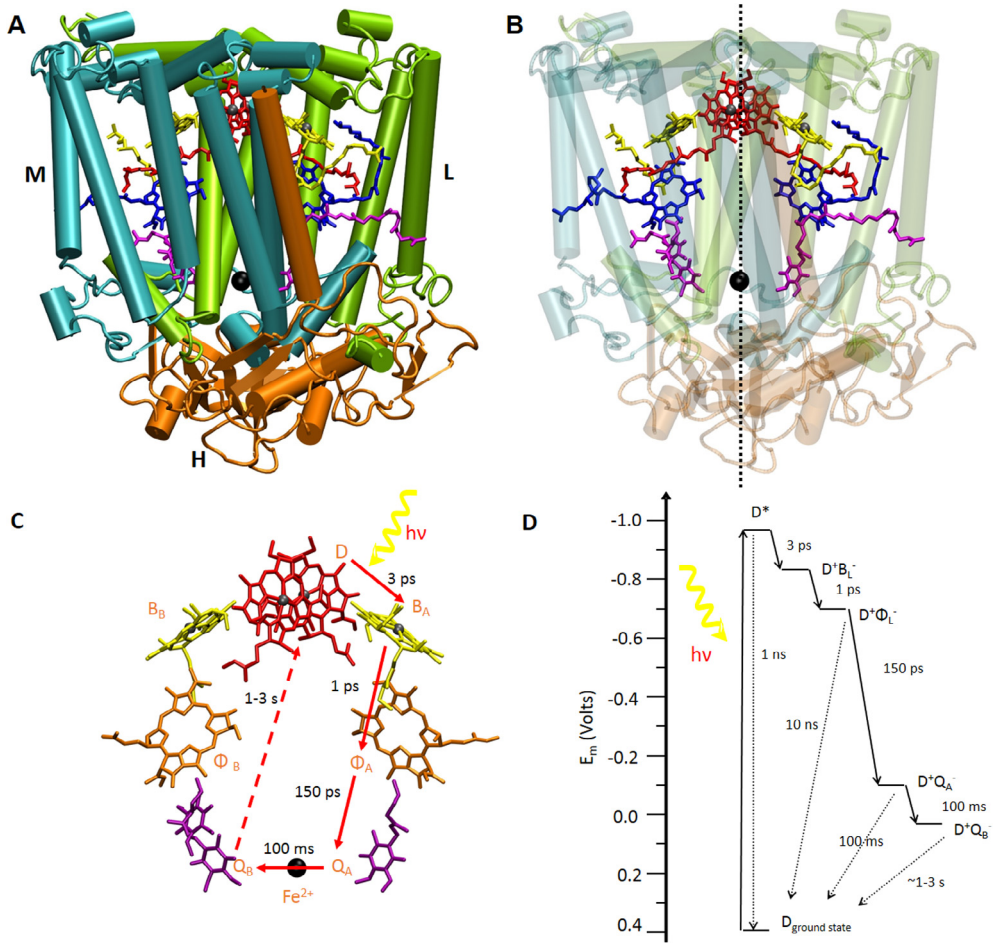

Fig. 1. Crystallographic structure of the RC from *R. sphaeroides* strain R-26 and diagram of light-induced electron transfer. (A) The three subunits L (cyan), M (green), and H (orange). The H polypeptide has an extra-membrane domain, at the cytoplasmic side of the plasma membrane. (B) Cofactors arrangement within the protein scaffold. Cofactors are shown as sticks, with Mg and Fe atoms as gray or black spheres, respectively. The dotted vertical line represents the 2-fold symmetry axle. (C) Detail of cofactor and light-induced electron transfer reaction. Side chains have been cut for clarity. The BChl dimer (D) is colored in red, the two monomeric BChls (B) are yellow, BPhes (Φ) are blue, the two UQ_{10} are violet. All cofactors are arranged in two branches (called A and B) around an axis of twofold pseudo-symmetry. Solid arrows indicate the forward electron transfer while dashed arrow indicates the charge recombination. (D) Energetic diagram of the light-induced electron transfer with indication of time constant of each reaction. The figure was constructed using PDB file 1AIJ [30]. (For interpretation of the references to color in this figure legend, the reader is referred to the web version of this article.)

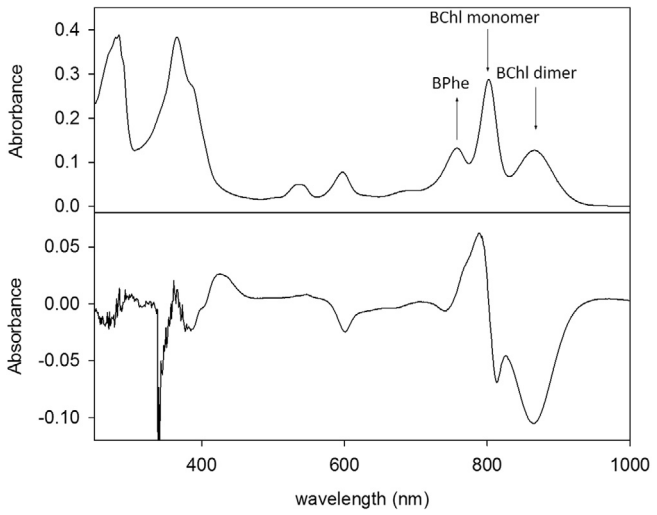

Fig. 2. Upper panel: absorption spectrum of purified RC 1 μM dissolved in TLE buffer; lower panel: light-dark spectrum obtained by cross-illuminating the RC with an high power violet light during spectrum scan. Arrows indicate how spectrum modifies upon denaturation.

tion of 1.87 Å [31]. Moreover, RC features several absorption peaks spanning the spectral range from the UV to the NIR that allow to assess easily its integrity. In particular, the dimer absorption band around 865 nm arises from the excitonic coupling of two closely spaced Bchls and the position of its maximum is very sensitive to the protein surrounding. Other phenomena related to the denaturation are the loss of the central magnesium from the bacteriochlorophylls, i.e. the pheophytinization of the BChls, and the release of the bacteriochlorins from the protein scaffolding. Both effects lead to a decrease of the 800 nm band (associated to the BChls) and an increase of the 755 nm band (associated to the BPhs), often associated to a blue shift when they are released from the protein (Fig. 2, upper panel).

Under irradiation, the isolated RCs is bleached as the electron sitting in the dimer is shuttled to the final electron acceptor forming the $D^+Q_B^-$ state. The spectrum obtained under continuous illumination differs markedly from the spectrum of the protein in the ground state, and the changes are mainly due to the D/D^+ absorption changes (Fig. 2, lower panel). This characteristic difference between dark and light spectra offers a tool to study the protein photoactivity. Indeed, the charge-separated state can be also generated by a short and saturating light pulse, which promotes the protein in the D^+Q_B state. Immediately after the light pulse the charge-separated state recombines toward the ground state with an exponential kinetic that can be easily followed at any of the wavelengths of Fig. 2 (lower panel), including 865 nm, where the difference is maximum. In particular, the bleaching of the signal is proportional to the fraction of photoactive RC, as depicted in Fig. 3, lower panels.

The sonication-induced denaturation of RC have been studied in different environments: the LDAO micellar system; the liposome system (with three different lipid compositions), i.e. where the protein is routinely reconstituted to mimic the natural membrane; finally in a detergent-free buffer, in order to assess the surface-active molecule role in the ultrasound-protein interaction. All chemical compositions of the solubilizing solution tested, along with the characteristic protein denaturation time are listed in Table 1.

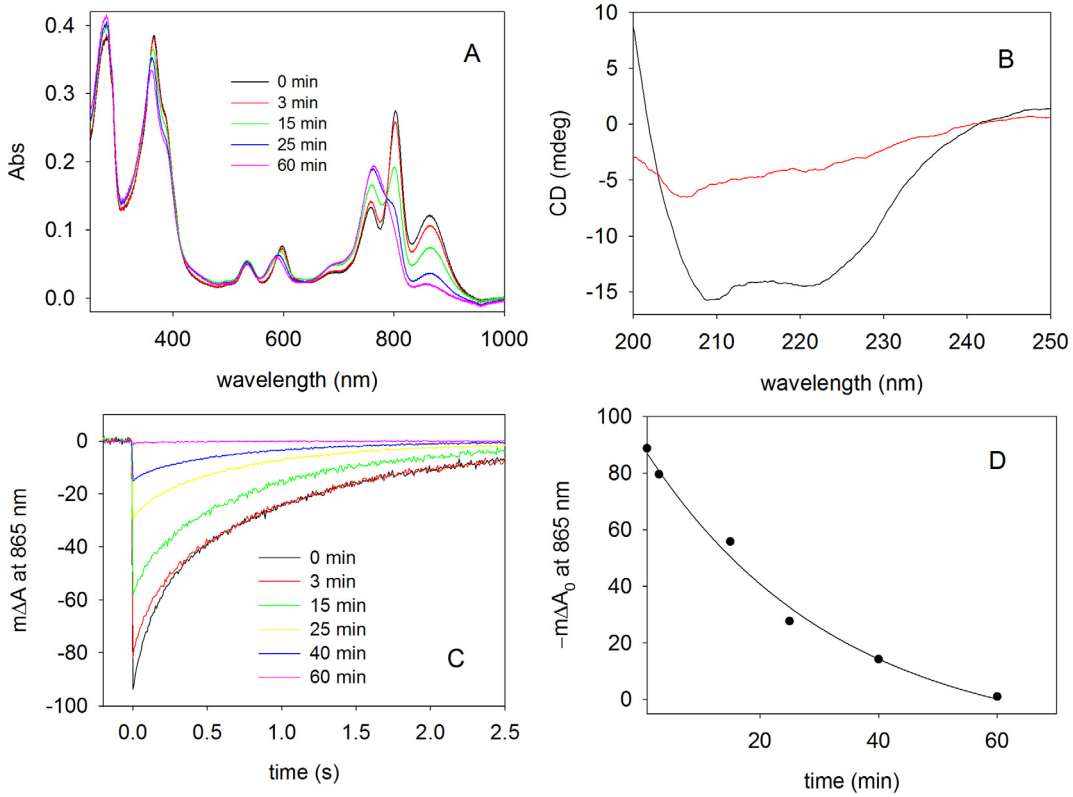

Fig. 3. Denaturation of RC in LDAO micelles (phosphate 50 mM, KCl 100 mM, LDAO 0.025%, pH 7.5). (A) Optical absorption spectra recorded after increasing sonication time as indicated in the legend. (B) CD spectra of native RC in detergent solution (black line) and after 60 min sonication (red line). (C) CR traces recorded after increasing sonication time as indicated in the legend. (D) Amplitude of the CR signal immediately after flash excitation as a function of sonication time. The line represents the monoexponential fitting of the experimental points. (For interpretation of the references to color in this figure legend, the reader is referred to the web version of this article.)

Table 1
summary of RC denaturation rate in different environments.

Sample	Detergent	Lipid(s) (Molar ratio)	Lifetime (min)
RC-micelles	LDAO	/	32 ± 4
RC-liposomes	/	PC	3.8 ± 1.0
RC-liposomes	/	PC:CL 4:1	6.5 ± 0.5
RC-liposomes	/	PC:CH 4:1	6.5 ± 0.5
Surfactant free RC-suspension	/	/	5.5 ± 1.5

3.1. Sonication of RC in LDAO micelles

A homogeneous solution of RC 1 μM in phosphate buffer pH 7.5 containing KCl 100 mM and LDAO 0.025% w/v (equal to its critical micellar concentration CMC) was subjected to cycles of sonication performed at 30 W constant power in pulsed modality as described in Section 2.4. Sample was kept in a water/ice bath to prevent overheating of the solution during sonication. Optical spectra of the protein rerecorded at regular time intervals (Fig. 3 A) show the modification of the chlorin pigments within the protein and are possibly associated to modification of the tertiary structure of the protein.

The absorption spectra of the RC is dramatically affected by sonication in its NIR region, while the effects are mitigate at lower wavelengths. In Fig. 3 A the peaks associated with the dimer D and the monomeric bacteriochlorophylls, at 865 and 800 nm respectively, lower their intensity during sonication while the peak at 755 nm, associated to bacteriopheophytin, increases its intensity and undergoes to a hypsochromic shift during the treatment. The loss of the central magnesium ion of the bacteriochlorophylls, which appears to be the most prominent sonication result on the pigments, induces the disassembly of the dimer – with the consequent loss of activity – and the overall increase in the BPhs content. The hypsochromic shift appears instead to be more closely related to the loss of the protein tertiary structure. Indeed, the release of the pigment toward the water bulk solution can take place only if the interaction between BPhs and the aminoacids is broken by sonication. Notwithstanding the fact that BPh is virtually insoluble in water, the presence of LDAO in solution probably plays a relevant role in stabilizing the pigment in an aqueous environment. These changes also reflect the blue-shift in the maximum of the smaller peak at 605 nm. It is noteworthy the absence of scattering increase in the optical spectra during sonication, which suggests that during the exposure to ultrasound, the proteins do not aggregates in the presence of the detergent LDAO.

The ultrasound-induced denaturation results irreversible as the spectra of the protein solution collected immediately after sonication was identical to the spectrum recorded after 24 h of storage at 5 °C (data not shown). A similar behavior was also found for RC denatured by thermal treatment [32], indicating that the loss of protein scaffold integrity has the same effect in both cases.

Circular dichroism (CD) spectra give complementary information to the optical spectra since they are related to the secondary structure of the proteins. RC has a well-known composition, featuring 54% α-helix, 11% β-sheet and 35% random coil and the relative amounts are expected to change upon denaturation [33]. Fig. 3 B shows the CD spectra of RC in LDAO micelles before and after the sonication experiment. The curve of RC in the native state (black line) agreed with the results previously obtained in similar

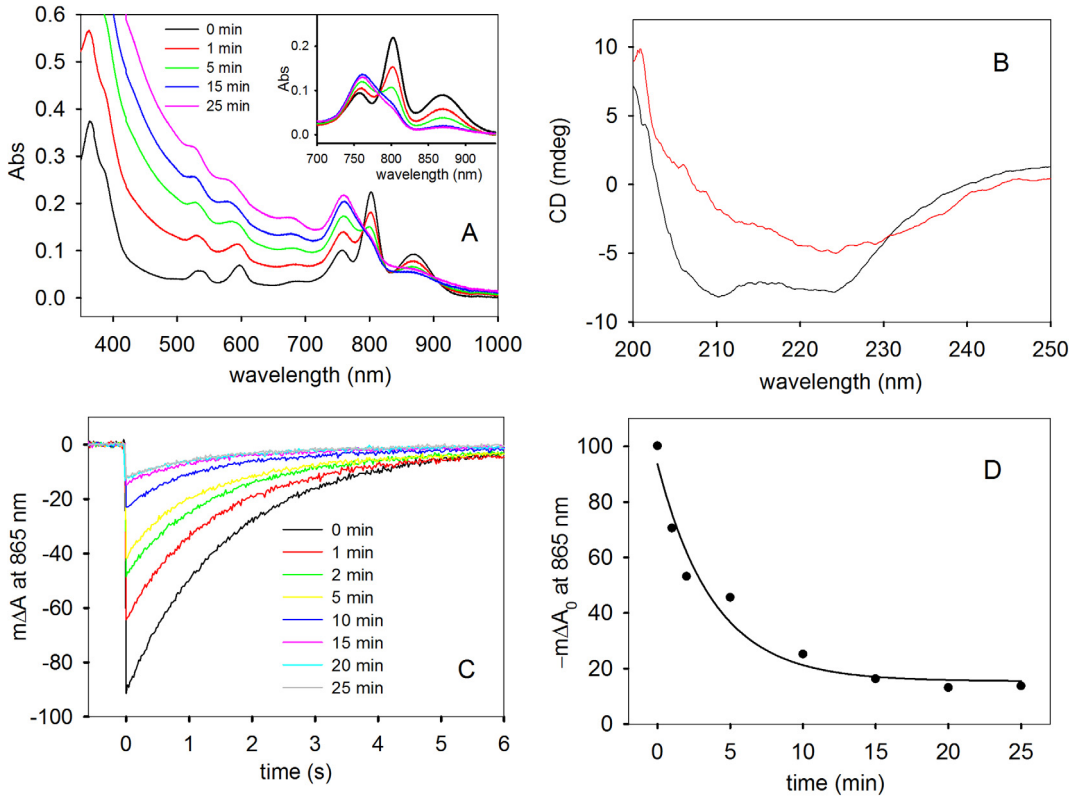

Fig. 4. Denaturation of 1 μM RC in POPC liposomes in phosphate 50 mM, KCl 100 mM, pH 7.5. (A) Optical absorption spectra recorded after increasing sonication time as indicated in the legend. Inset: NIR spectral region after subtracting the scattering contribution. (B) CD spectra of native RC in detergent solution (black line) and after 25 min sonication (red line). (C) CR traces recorded after increasing sonication time as indicated in the legend. (D) Amplitude of the CR signal immediately after flash excitation as a function of sonication time. The line represents the monoexponential fitting of the experimental points. (For interpretation of the references to color in this figure legend, the reader is referred to the web version of this article.)

conditions [34], while the curve of the 60 min sonicated sample (red line) indicates that the secondary structure of the protein is lost, similarly to what found for the thermal denaturation [33]. This result is in agreement with the optical spectra, since the pigments are embedded within the transmembrane helices of the protein, and the loss of the tertiary and, even more, the secondary structure features are responsible for the release of the pigments outside the protein.

Photochemical activity was finally determined by recording the flash-induced absorption changes at 865 nm that reflect the formation of the charge-separated state $DQ \rightarrow D^{+}Q^{-}$ and its subsequent CR kinetics (see Section 3). The decreasing amplitude of these signals is related to the loss of photochemical activity, i.e. due to the decrease of the proteins fraction capable to generate the charge-separated state. The charge recombination kinetics of RC recorded at increasing sonication time are shown in Fig. 3 C, while in Fig. 3 D the amplitude of the signal immediately after the flash pulse is presented as function of sonication time. The experimental points were fitted to a monoexponential function and a lifetime for the photoactivity loss of 32 ± 4 min was obtained.

3.2. Sonication of RC reconstituted in proteoliposomes

RCs were reconstituted in membrane-mimicking lipid vesicles by the MVT method, a very efficient technique to prepare phospholipid-based proteoliposomes. The lipid-to-protein molar ratio was kept constant to 1000:1, while the lipid formulation was varied: i) pure phosphatidylcholine (PC), ii) PC/cardiolipin (CL) 4:1 and iii) PC/cholesterol (CH) 4:1 mixtures were respectively prepared. The proteoliposomes suspensions were then sonicated and analyzed in a similar way to the RC in LDAO micelles (Section 3.1).

For RC reconstituted in proteoliposomes of pure PC we observed a progressive denaturation and loss of photoactivity with the increase in sonication time (Fig. 4 A and C) like the case of the RC in LDAO micelles. Remarkably, the denaturation lifetime of RC in PC liposomes (Fig. 4 D) was 3.8 ± 1.0 min, roughly ten-time faster than in LDAO micelles. Furthermore, the absorption spectra in Fig. 4 A show a significant increase of the solution scattering which indicates protein aggregation as previously found for the case of thermal denaturation [34]. CD spectra (Fig. 4 B) show that the secondary structure of the native protein is very similar in liposomes and in LDAO micelles, while after the sonication the spectra become quite different suggesting that the denaturation progresses toward different final states in the two environments.

At first sight, the experimental evidence that the RC denaturation is much faster in liposomes rather than in detergent can appear surprising. In fact, the liposomes are small, vesicular lipid membranes mimicking properties and functions of native cell membranes and therefore one might expect a greater resistance of RC embedded in vesicles during sonication. Several hypotheses can be proposed to justify this outcome. The first one stems from the consideration that when sonication occurs in a solution of surface-active molecules, cavitation process is inevitably affected. Surfactant molecules indeed, accumulate at the gas/liquid interface of the cavitating bubble, thus reducing the surface tension. Consequently an enhanced formation rate of the bubbles occurs. On the other hand, surfactants at the water/gas interface bring about to a decayed bubble fusion rate, thus inducing a smaller size of cavitating bubbles [7,35–38]. Then, in the presence of surfactants, the

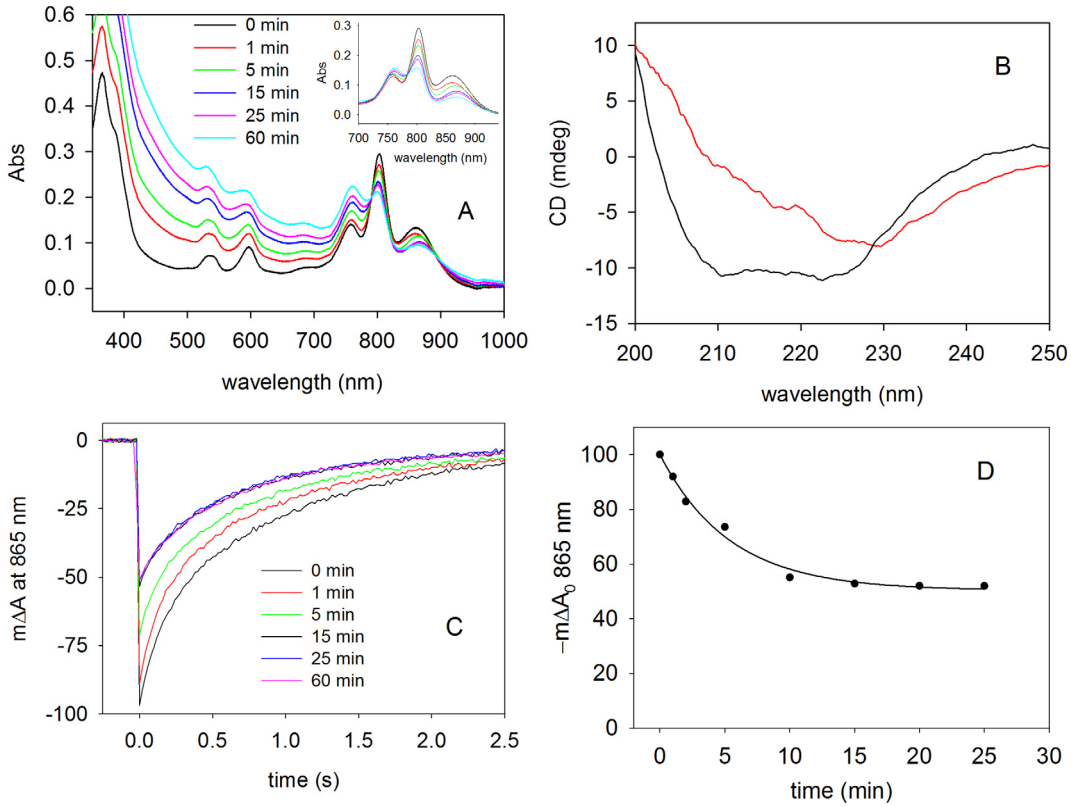

Fig. 5. Denaturation of RC in detergent-free buffer (phosphate 50 mM, KCl 100 mM, pH 7.5). (A) Optical absorption spectra recorded after increasing sonication time as indicated in the legend. Inset: NIR spectral region after subtracting the scattering contribution. (B) CD spectra of native RC in detergent-free buffer (black line) and after 25 min sonication (red line). (C) CR traces recorded after increasing sonication time as indicated in the legend. (D) Amplitude of the CR signal immediately after flash excitation as a function of sonication time. The line represents the monoexponential fitting of the experimental points. (For interpretation of the references to color in this figure legend, the reader is referred to the web version of this article.)

cavitation effects are less marked, and the interaction with living matter less effective. Also lipids are surfactant molecules to a certain extent, but the critical aggregation concentration (CAC) in water is about 1–2 mM for LDAO [39] and about 4–5 μM for PC [40]. Therefore, at or above the CAC, the number of monomers of PC in solution is negligible [41], as well as the effect on the surface tension of the water. This could cause a lower efficacy of cavitation in LDAO compared to PC solutions. Furthermore, during the experiments conducted in solution of LDAO, the sonicator horn was surrounded by a stable layer of foam that definitely has restricted the effective transmission of ultrasound to the bulk of the solution [42]. In addition to these effects, the ultrasound-generated free radicals in phosphatidylcholine liposomes should be considered [43]. Indeed, oxygen radicals and some lipid peroxidation products, derived from the unsaturated fatty acid chains of lipids exposed to ultrasound, could significantly contribute to the RC injury when embedded in proteoliposomes. Obviously, these and other phenomena can synergistically act on the RC denaturation process in liposomes, and further studies are needed to determine in detail their mechanism of action and effectiveness.

In the case of RC reconstituted in the mixtures PC:CL 4:1 and in PC:CH 4:1 the optical absorption and CD spectral variations closely resemble those obtained in the case of PC alone and hence not shown. However, the lifetime for the loss of photoactivity was 6.5 ± 0.5 min for both the proteoliposomes, almost twice as much as measured in vesicles made only of PC. CL, or bisphosphatidylglycerol, is an acidic phospholipid known to establish strong interactions with the RC of photosynthetic bacteria, influencing the protein structure and function, and affecting RC thermal stability and photodegradation or photooxidation damage, as previously reported for *R. sphaeroides* by Jones et al. [44] and De Leo et al. [45]. On the other hand CH is a lipid constituent of biological membranes with the ability to modulate some membrane properties such as fluidity and permeability. In particular, CH reduces membrane fluidity above the phase transition temperature, with a corresponding reduction in permeability to aqueous solutions, and increases the fluidity of membranes below the phase transition temperature [32]. Moreover, CH can intercalate among the constituents of the bilayer and then can fill in the gaps among lipid molecules and integral proteins embedded in the membrane. Therefore, both CL and CH could stabilize RC structurally, somewhat mitigating the effects of sonication and slowing down the denaturation process.

3.3. Sonication of RC in surfactant free buffer

A final set of measurements was carried out with RC 1 μM in phosphate 50 mM, KCl 100 mM pH 7.5. In this detergent-free buffer, the only detergent present in the system is the residual LDAO coming from the RC stock solution, i.e. about 0.001%. Analyzing the absorption spectra and the kinetics of charge recombination realized in function of the sonication time (Fig. 5 A and C) we note a similarity of results with denaturation experiments conducted in liposomes. The denaturing lifetime obtained from CR kinetics was found to be 5.5 ± 1.5 min (Fig. 5 D), similar to that obtained in the proteoliposomes.

An increase of the solution scattering is also observed during the denaturation experiments, making the behavior of this sample similar to that of proteoliposomes and different to that one of RC in LDAO micelles. CD spectra (Fig. 5 B) show, also in this case, that the secondary structure is heavily perturbed at the end of the sonication process.

Another interesting feature in this experiment is that even after 60 min sonication time, about 50% of the protein remains photoactive, possibly indicating that the aggregation induced by sonication protects the RC from further denaturation (see Section 3.4).

3.4. Ultrasound induced RC aggregation

The turbidity increase in sonicated solution of RC in proteoliposomes and detergent-free buffer probably originates from two different phenomena. In the case of the phospholipid vesicles we can expect that sonication pours energy on the lipid system and that most of the scattering recorded in the UV region may arise from the reorganization of vesicles. In the case of detergent-free buffer, the aggregation is a direct consequence of the highly hydrophobic nature of the LM subunits which, to minimize the interaction with water, tend to self-organize in large aggregates [46]. On the contrary, when the RC is embedded in LDAO micelles

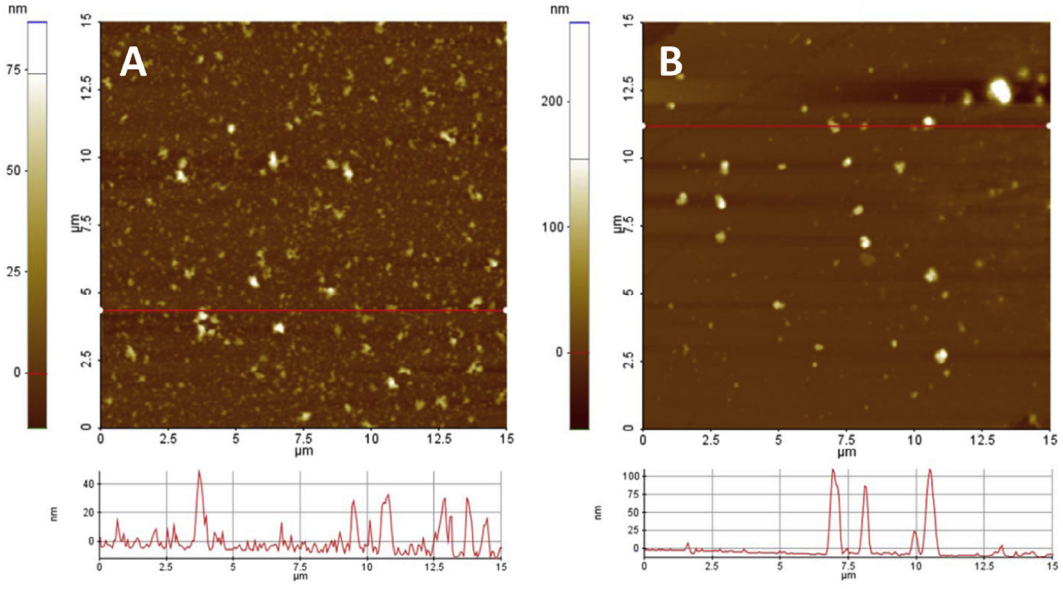

Fig. 6. Denaturation of RC in detergent-free buffer. Height AFM micrographs and corresponding height profiles of RC deposited onto mica, before (A) and after (B) the sonication experiment (30 min). Scan size is 15 μm × 15 μm.

no turbidity increase was observed, differently from what observed for thermal induced denaturation in similar conditions [34].

Atomic force microscopy characterization of protein aggregation phenomena induced by the sonication was carried out on aliquots of the same RC sample deposited onto mica before and after (Fig. 6 A and B respectively) the sonication treatment in detergent-free buffer. The two conditions show dramatic morphological differences. In particular solutions unexposed to sonication show numerous and spread objects, with the majority of them having a height profile ranging between 10 and 30 nm, indicating the presence of small but numerous entities. Conversely, in sonicated RC, fewer objects are visible having heights of about 100 nm revealing the formation of large aggregates induced by the sonication, in agreement with the scattering increase already observed in solution. Since about 50% of the RC remains photoactive when sonicated in detergent-free buffer even after long treatment times (Section 3.3), we hypothesize the existence of unperturbed proteins within the core of these aggregates, probably shielded by the surrounding proteinaceous material.

4. Conclusions

The experimental evidences gathered in this work strongly indicate that integral membrane proteins denature and suffer a significant extent of activity loss under ultrasound treatment.

The photosynthetic RC, a photochemically active membrane protein used as integral membrane protein model, during sonication loses its ability to absorb and convert light energy in a charge-separated state. Such loss takes place with different magnitudes depending on the medium in which the protein is dispersed. Denaturation occurs much faster when the RC is solubilized in membrane-mimicking proteoliposomes than in detergent micelles. Such finding can be rationalized based on the cavitation effects, which seem less effective in the presence of LDAO detergent with respect to lipids, and on the formation of lipid peroxidation products in proteoliposomes.

Interestingly enough, detergent-free RCs tend to form large aggregates during sonication, probably resulting in a protecting structure from further denaturation.

Acknowledgments

This work was supported by the financial contribution of PRIN 2010–2011 “Organizzazione Funzionale a Livello Nanoscopico di (Bio)Molecole e Ibridi per Applicazioni nel Campo della Sensoristica, della Medicina e delle Biotecnologie”.

References

[1] P.B. Stathopulos, G.A. Scholz, Y.-M. Hwang, J.A.O. Rumfeldt, J.R. Lepock, E.M. Meiering, Sonication of proteins causes formation of aggregates that resemble amyloid, Protein Sci. 13 (2004) 3017–3027.
[2] M. Villamiel, P. De Jong, Influence of high intensity US and heat treatment in continuous flow in fat, proteins and native enzymes of milk, J. Agric. Food Chem. 48 (2000) 472–478.
[3] R. Bhaskaracharya, S. Kentish, M. Ashokkumar, Selected applications of ultrasonics in food processing, Food Eng. Rev. 1 (2009) 31–49.
[4] M. Ashokkumar, D. Sunartio, S. Kentish, R. Mawson, L. Simons, K. Vilkhu, C. Versteeg, Modification of food ingredients by US to improve functionality: a preliminary study on a model system, Innovative Food Sci. Emerg. Technol. 9 (2008) 155–160.
[5] C. Yan, J.H. Resau, J. Hewetson, M. West, W.L. Rill, M. Kende, Characterization and morphological analysis of protein-loaded poly(lactide-co-glycolide) microparticles prepared by water-in-oil-in-water emulsion technique, J. Cont. Rel. 32 (1994) 231–241.
[6] R. Krishnamurthy, J.A. Lumpkin, R. Sridhar, Inactivation of lysozyme by sonication under conditions relevant to microencapsulation, Int. J. Pharm. 205 (2000) 23–34.
[7] A. Schroedera, J. Kostb, Y. Barenholza, Ultrasound, liposomes, and drug delivery: principles for using ultrasound to control the release of drugs from liposomes, Chem. Phys. Lipids 162 (2009) 1–16.
[8] A.U. Kapturowska, I.A. Stolarzewicz, J. Krzyczkowska, E. Białecka-Florjanczyk, Studies on the lipolytic activity of sonicated enzymes from Yarrowia lipolytica, Ultrason. Sonochem. 19 (2012) 186–191.
[9] Y. Chisti, Sonobioreactors: using ultrasound for enhanced microbial productivity, Trends Biotechnol. 21 (2003) 89–93.
[10] G.P. Saborio, B. Permanne, C. Soto, Sensitive detection of pathological prion protein by cyclic amplification of protein misfolding, Nature 411 (2001) 810–813.
[11] D.A. Lomas, R.W. Carrell, Serpinopathies and the conformational dementias, Nat. Rev. Genet. 3 (2002) 759–768.
[12] M.A. Margulis, Sonochemistry and Cavitation, Gordon and Breach Science Publishers, Amsterdam, 1995.
[13] F.R. Young, Cavitation, McGraw-Hill, Maidenhead, 1989.
[14] P. Riesz, T. Kondo, Free radical formation induced by ultrasound and its biological implications, Free Radical Biol. Med. 13 (1992) 247–270.
[15] M. Di Marco, S. Shamsuddin, K.A. Razak, A.A. Aziz, C. Devaux, E. Borghi, L. Laurent, C. Sadun, Overview of the main methods used to combine proteins with nanosystems: absorption, bioconjugation, and encapsulation, Int. J. Nanomed. 5 (2010) 37–49.
[16] C.L. Hawkins, M.J. Davies, Generation and propagation of radical reactions on proteins, Biochim. Biophys. Acta 1504 (2001) 196–219.
[17] T.J. Mason, D. Peters, Practical sonochemistry: uses and applications of ultrasound, 2nd ed., Horwood Publishing, Chichester, West Sussex, UK, 2002.
[18] Z.M. Tian, M.X. Wan, S.P. Wang, J.Q. Kang, Effects of ultrasound and additives on the function and structure of trypsin, Ultrason. Sonochem. 11 (2004) 399–404.
[19] Y. Ohhashi, M. Kihara, H. Naiki, Y. Goto, Ultrasonication-induced Amyloid Fibril Formation of β2-Microglobulin, J. Biol. Chem. 280 (2005) 32843–32848.
[20] J. Chandrapala, B. Zisu, M. Palmer, S. Kentish, M. Ashokkumar, Effects of ultrasound on the thermal and structural characteristics of proteins in reconstituted whey protein concentrate, Ultrason. Sonochem. 18 (2011) 951–957.
[21] B. Kwiatkowska, J. Bennett, J. Akunna, G.M. Walker, D.H. Bremner, Stimulation of bioprocesses by ultrasound, Biotechnol. Adv. 29 (2011) 768–780.
[22] Structural Genomics on Membrane Proteins, CRC Press, Boca Raton, 2006.
[23] E. Wallin, G. Von Heijne, Genome-wide analysis of integral membrane proteins from eubacterial, archaean, and eukaryotic organisms, Protein Sci. 7 (1998) 1029–1038.
[24] E.N. Lyukmanova, Z.O. Shenkarev, N.F. Khabibullina, G.S. Kopeina, M.A. Shulepko, A.S. Paramonov, K.S. Mineev, R.V. Tikhonov, L.N. Shingarova, L.E. Petrovskaya, D.A. Dolgikh, A.S. Arseniev, M.P. Kirpichnikov, Lipid–protein nanodiscs for cell-free production of integral membrane proteins in a soluble and folded state: Comparison with detergent micelles, bicelles and liposomes, Biochim. Biophys. Acta 2012 (1818) 349–358.
[25] L. Catucci, V. De Leo, F. Milano, L. Giotta, R. Vitale, A. Agostiano, A. Corcelli, Oxidoreductase activity of chromatophores and purified cytochrome bc 1 complex from Rhodobacter sphaeroides: a possible role of cardiolipin, J. Bioenerg. Biomembr. 44 (2012) 487–493.
[26] R.R. Tangorra, A. Operamolla, F. Milano, O.H. Omar, J. Henrard, R. Comparelli, F. Italiano, A. Agostiano, V. De Leo, R. Marotta, A. Falqui, G.M. Farinola, M. Trotta, Assembly of a photosynthetic reaction center with ABA tri-block polymersomes: highlights on protein localization, Photochem. Photobiol. Sci. 14 (2015) 1844–1852.
[27] V. De Leo, L. Catucci, A. Falqui, R. Marotta, M. Striccoli, A. Agostiano, R. Comparelli, F. Milano, Hybrid assemblies of fluorescent nanocrystals and membrane proteins in liposomes, Langmuir 30 (2014) 1599–1608.
[28] F. Milano, A. Agostiano, F. Mavelli, M. Trotta, Kinetics of the quinone binding reaction at the Q(B) site of reaction centers from the purple bacteria Rhodobacter sphaeroides reconstituted in liposomes, Eur. J. Biochem. 270 (2003) 4595–4605.
[29] M. Roth, A. Lewit-Bentley, H. Michel, J. Deisenhofer, R. Huber, D. Oesterhelt, Detergent structure in crystals of a bacterial photosynthetic reaction centre, Nature 340 (1989) 659–662.
[30] M.H.B. Stowell, T.M. McPhillips, D.C. Rees, S.M. Soltis, E. Abresch, G. Feher, Light-induced structural changes in photosynthetic reaction center: Implications for mechanism of electron-proton transfer, Science 276 (1997) 812–816.
[31] J. Koepke, E.-M. Krammer, A.R. Klingen, P. Sebban, G.M. Ullmann, G. Fritzsch, PH modulates the quinone position in the photosynthetic reaction center from Rhodobacter sphaeroides in the neutral and charge separated states, J Mol Biol 371 (2007) 396–409.
[32] Liposomes as Tools in Basic Research and Industry, CRC Press, Boca Raton, 1994.
[33] C. Nicolini, V. Erokhin, F. Antolini, P. Catasti, P. Facci, Thermal stability of protein secondary structure in Langmuir-Blodgett films, Biochim. Biophys. Acta 1158 (1993) 273–278.
[34] M. Ishimura, S. Honda, H. Uedaira, T. Odahara, J. Miyake, Thermal denaturation of photosynthetic membrane proteins from Rhodobacter sphaeroides, Thermochim. Acta 266 (1995) 355–364.
[35] M. Ashokkumar, F. Grieser, The effect of surface active solutes on bubbles in an acoustic field, Phys. Chem. Chem. Phys. 9 (2007) 5631–5643.
[36] L.A. Crum, Measurements of the growth of air bubbles by rectified diffusion, J. Acoust. Soc. Am. 68 (1980) 203–211.

[37] B. Jimmy, S. Kentish, F. Grieser, M. Ashokkumar, Ultrasonic nebulization in aqueous solutions and the role of interfacial adsorption dynamics in surfactant enrichment, Langmuir 24 (2008) 10133–10137.
[38] D. Sunartio, M. Ashokkumar, F. Grieser, Study of the Coalescence of Acoustic Bubbles as a Function of Frequency, Power, and Water-Soluble Additives, J. Am. Chem. Soc. 129 (2007) 6031–6036.
[39] K.W. Herrmann, Non-ionic—cationic micellar properties of dimethyldodecylamine oxide, J. Phys. Chem. 66 (1962) 295–300.
[40] Cis-trans Isomerization in Biochemistry, Wiley-VCH, Weinheime, 2006.
[41] T.F. Zhu, J.W. Szostak, Preparation of large monodisperse vesicles, PLoS ONE 4 (2009) e5009.
[42] N.M. Tole, Interaction of ultrasound with matter, in: H. Ostensen (Ed.), Basic Physics of Ultrasonographic Imaging, WHO Press, Geneva, 2005.
[43] R. Maffei Facino, M. Carini, G. Aldini, L. Saibene, A. Macciocchi, Antioxidant profile of nimesulide, indomethacin and diclofenac in phosphatidylcholine liposomes (PCL) as membrane model, Int. J. Tissue React. 15 (1993) 225–234.
[44] M.R. Jones, P.K. Fyfe, A.W. Roszak, N.W. Isaacs, R.J. Cogdell, Protein–lipid interactions in the purple bacterial reaction centre, Biochim. Biophys. Acta 1565 (2002) 206–214.
[45] V. De Leo, L. Catucci, A. Ventrella, F. Milano, A. Agostiano, A. Corcelli, Cardiolipin increases in chromatophores isolated from Rhodobacter sphaeroides after osmotic stress: structural and functional roles, J. Lipid Res. 50 (2009) 256–264.
[46] P. Gast, P.W. Hemelrijk, H.J. VanGorkom, A.J. Hoff, The association of different detergents with the photosynthetic reaction center protein of Rhodobacter sphaeroides R26 and the effects on its phytochemistry, Prog. Biophys. Mol. Biol. 65 (1996) Pe109.